Paramagnetic relaxation resonance of optically oriented metastable He^4 atoms in an effective magnetic field

A. I. Okunevich

A. F. Ioffe Physico-technical Institute, USSR Academy of Sciences
(Submitted March 12, 1974)
Zh. Eksp. Teor. Fiz. **67**, 881–889 (September 1974)

Experiments were performed with modulation of the discharge intensity and at optical orientation of the metastable He^4 atoms under magnetic-resonance conditions. It is found that the relaxation modulation that arises in this case results in resonant variation of the absorption of the pumping light when the nutation frequency ω_1 is equal to the modulation frequency and also when $\omega_1=0$. The observed resonance signals are identified as the previously predicted relaxation resonance signals. A detailed comparison of the properties of the observed signals with the theory is carried out.

It was shown in an earlier paper[1], on the basis of solutions of the Bloch equation, that modulation of the relaxation of optically-oriented atoms in a transverse magnetic field leads to a resonant change of the magnetic moment of an ensemble of atoms when the modulation frequency coincides with the Larmor frequency or its subharmonics. This phenomenon was called parametric relaxation resonance. In addition, it was shown that a similar phenomenon should occur for optically-oriented atoms under the conditions of ordinary magnetic resonance. In this case, the role of the transverse magnetic field is played by the effective magnetic field, and relaxation resonance should be observed when the relaxation-modulation frequency coincides with the nutation frequency or its subharmonics.

This paper reports observation of parametric relaxation resonance in an effective magnetic field for optically-oriented He^4 atoms in the metastable 2^3S_1 state. The relaxation was modulated by using the dependence of the relaxation rate in helium on the electric-discharge intensity[2]. The properties of the observed resonance signals were investigated and the results were compared with theory.

1. EXPERIMENTAL TECHNIQUE AND PROCEDURE

In the experiment we registered the change of the absorption of the pump light propagating along a constant magnetic field H_0 parallel to the z axis. It is known that the resultant optical-detection signal is proportional to the projection M_z of the magnetic moment of the ensemble of atoms. A theoretical analysis[1] shows that at a relaxation-modulation frequency Ω there are produced components M_z that oscillate at frequencies $n\Omega$ and vary in resonant fashion when the condition $\omega_1 = k\Omega$ is satisfied (here $\omega_1 = \gamma H_1$ is the nutation frequency). In our experiments, we detected the M_z component oscillating at the frequency Ω.

The main difficulty was that when the high-frequency that the optical radiation from the cell is modulated maintains the discharge is modulated at the frequency Ω. To eliminate the influence of this parasitic modulation, we used pulsed amplitude modulation of a radio-frequency resonant magnetic field H_1 at a low frequency F. After synchronous detection of the oscillations of frequency Ω, the useful signal of frequency F was amplified, synchronously detected again, and then fed to the automatic recorder.

Figure 1. shows a block diagram of the experimental setup. The light source was a helium capillary lamp 1, in which a high-frequency electrodeless capacitive discharge was excited with the aid of generator 2 (frequency 31 MHz). The light from the lamp was gathered into a parallel beam by means of a lens 3, and then, after passing through a polaroid 4 and a quarter-wave plate (see 5), it became circularly polarized and was fed to a spherical absorbing cell 6 filled with helium at pressure 0.8 Torr (cell diameter 5 cm). The change of the absorption of the light after passing through cell 6, interference filter 7, and focusing lens 8 was registered with a photoreceiver 9. The interference filter had a transmission maximum at the wavelength $\lambda = 1.08$ μ corresponding to the transition from the metastable 2^3S_1 state to the 2^3P state of orthohelium. The photoreceiver was an FD-7K photodiode.

A high-frequency capacitive electrodeless discharge was maintained in absorbing cell 6 with the aid of a type G4-68 generator 12 (frequency 28 MHz). Annular slotted electrodes were used to produce the discharge. They were secured directly to the cell and produced an electric high-frequency field directed parallel to the pump light beam. The voltage of generator 12 was amplitude-modulated at a frequency Ω with the aid of generator 13. The optical-detection signal from the output of the photoreceiver 9 was fed to a narrow-band amplifier 10 tuned to the frequency Ω. The output signal of this amplifier was fed to synchronous detector 11. The reference voltage in this detector was the voltage of the generator 13. The time constant of the detector 11 was 13.6 msec and was chosen such as to pass to the output of detector 11 the low-frequency signal envelope of frequency F. The signal from the detector output was fed to the input of the amplifier 14, tuned to the frequency F. After amplification, the signal was fed to the synchronous detector 15. The reference voltage for this detector was the voltage of the generator 16, which amplitude-modulated the radio-frequency magnetic field at a frequency F = 18 Hz.

The radiofrequency resonant magnetic field $2H_1$ was produced with the aid of Helmholtz coils 17 (26 cm diameter). The field $2H_1$ was directed along the y axis and its frequency was ω. The voltage with frequency ω was produced by generator 18 and was fed to the radio-frequency rings 17 through an attenuator-modulator and a power amplifier (the latter is not shown in Fig. 1). The

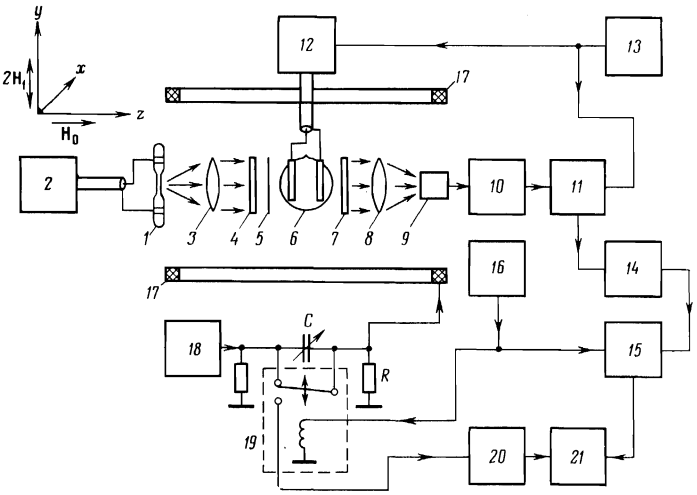

FIG. 1. Block diagram of experimental setup.

attenuator-modulator consisted of an RC attenuator with variable capacitance C and a commutating switch 19. The commutating switch was a VPM-1 vibrator-converter controlled by a voltage of frequency F from generator 16. When set in the upper position, the switch 19 shunted the capacitor C, and the total output voltage U_{max} of generator 18 was applied to the radio-frequency rings. When the switch was in the lower position, the voltage U applied to the rings, was lower and its value depended on the value of the capacitance C. This voltage was simultaneously fed to the amplitude detector 20. The output voltage of detector 20, which was proportional to the voltage U, was fed to the X input of automatic x-y plotter 21. The Y input of this plotter was the output of the synchronous detector 15. The time constant of detector 15 was 1 sec.

The capacitance C consisted of a bank of variable capacitors, and could be varied continuously with an electric motor that turned the rotor of the capacitor block. This varied the voltage U from $U \approx U_{max}$ to $U = U_{min}$, and changed the RF magnetic field H_1 from 15 to 0.2 mOe.

All the elements of the optical system, together with the RF rings, were mounted on an optical bench oriented along the earth's magnetic field. In addition, the auxiliary Helmholtz coils were fastened securely to the optical bench. The axis of these coils coincided with the direction of the light beam. These coils were used to modulate the magnetic field during the observation of the usual magnetic-resonance signal (S_z signal).

When the relaxation-resonance signals were observed, the tuning-to-zero condition $\Delta\omega = \omega - \omega_0 = 0$ was always satisfied. To satisfy this condition, the system was tuned beforehand to the center of the S_z-signal line by the following procedure: The auxiliary Helmholtz coils produced a low-frequency alternating field H_m of frequency 18 Hz and amplitude 0.5 mOe. The optical-detection signal, proportional to the derivative of the S_z signal, was fed from the output of photoreceiver 9 through amplifier 14 to synchronous detector 15. Neither the discharge nor the RF magnetic field were modulated in that case. The frequency was chosen such that the output voltage of the synchronous detector 15 was zero. The tuning accuracy was not less than 100 Hz. The change in the earth's magnetic field during the registration of the relaxation resonances did not exceed 0.03 mOe.

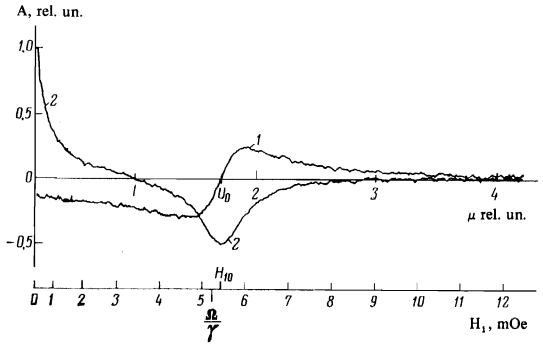

FIG. 2. In-phase (1) and quadrature (2) component of the optical-detection signal following modulation of the relaxation in He^4 ($\Omega/2\pi$ = 14.7 kHz, $\Delta\omega = 0$).

The generator 18 producing the resonant RF magnetic field was a GZ-49 quartz oscillator with frequency doubler at the output. The frequency doubler was used to broaden the frequency range of the generator. The frequency $\omega/2\pi$ of the resonant magnetic field was determined by the value of the earth's magnetic field (0.5 Oe) and was equal to 1.4 MHz. The frequency $\omega/2\pi$ could be varied discretely in steps of 2 Hz. The objective characteristics of the discharge intensity in the absorbing cell were the following: 1) the absorption $\Delta I/I$ of the pump light (λ = 1.08 μ) by the metastable He atoms, 2) the luminosity $\bar{I}_c$ of the discharge in the cell at the wavelength λ = 1.08 μ. The values of $\Delta I/I$ and $\bar{I}_c$ were calculated from the formulas

$$\frac{\Delta I}{I} = \frac{I_{ld} - I_{lcd}}{I_{ld} - I_d}, \qquad \bar{I}_c = I_{cd} - I_d.$$

These formulas contain the dc components of the current from the photo-receiver 9, namely the dark current I_d that flows when the lamp 1 and cell 6 are disconnected, the current I_{ld} with the lamp turned on and the cell disconnected, the current I_{cd} with the lamp turned off and the cell connected, and the current I_{lcd} with the lamp and cell both connected simultaneously.

The inhomogeneity of the constant magnetic field in the region of the cell was 0.1 mOe/cm. It was measured from the shift of the center of the S_z-signal line following a displacement of the absorbing cell. The entire measuring apparatus was located 5 meters away from the optical bench with the absorbing cell. To decrease the inhomogeneity of the magnetic field and the magnetic noise, all the experiments were performed on a nonmagnetic shielding base.

2. EXPERIMENTAL RESULTS AND DISCUSSION

Figure 2 shows the experimentally obtained plots of the optical- detection signals following modulation of the discharge intensity in the absorbing cell with optically oriented metastable He^4 under magnetic-resonance conditions ($\omega = \omega_0$). The abscissas in Fig. 2 represent the voltage U at the output of the attenuator-modulator (see Fig. 1). The voltage U is directly proportional to the amplitude H_1 of the resonant circularly-polarized component of the RF magnetic field. Figure 2 shows two plots obtained at different phases of the reference voltage in the synchronous detector 11 (see Fig. 1). The phase of the reference voltage was tuned in such a way that the signal was maximal at U = 0. Curve 2 was plotted at the obtained value of the phase, while curve 1 was plotted after shifting the phase by 90°.

To compare the observed signals with the relaxation-resonance signals predicted by the theory[1], let us write out in explicit form the formulas for the component M_z, which oscillates at the frequency. From formulas (3) and (4) of[1], in which we put $\omega_0 = \omega_1$ and $n - k = \pm 1$, we obtain

$$M_z(\Omega) = \bar{M}_0 \Gamma_p \sum_{k=-\infty}^{\infty} (-1)^k I_k(\varkappa) \left\{ [I_{k+1}(\varkappa) - I_{k-1}(\varkappa)] \frac{(\omega_1 - k\Omega)\cos \Omega t}{(\bar{\Gamma}+\Gamma_p)^2 + (\omega_1 - k\Omega)^2} \right.$$
$$\left. - [I_{k+1}(\varkappa) + I_{k-1}(\varkappa)] \frac{(\bar{\Gamma}+\Gamma_p)\sin \Omega t}{(\bar{\Gamma}+\Gamma_p)^2 + (\omega_1 - k\Omega)^2} \right\} \quad (1)$$

where Γ_p is the pumping rate, $\bar{\Gamma}$ is the average value of the relaxation rate, $\omega_1 = \gamma H_1$ is the nutation frequency ($\gamma/2\pi = 2.8$ kHz/mOe), $\varkappa = \mu\bar{\Gamma}/\Omega$, and I_k is a Bessel function of imaginary argument. Here, as in[1], it is assumed that the modulation of the relaxation rate Γ is given by

$$\Gamma = \bar{\Gamma}(1 + \mu \cos \Omega t). \quad (2)$$

It follows from (1) that $M_z(\Omega)$ contains an in-phase component (terms $\sim \cos\Omega t$) and a quadrature component (terms $\sim \sin\Omega t$). The in-phase component is the sum of the dispersion curves centered at the points $\omega_1 = k\Omega$, while the quadrature component is the sum of the absorption curves centered at the same points. In formula (1), the terms with $k > 0$ describe the resonant variation of $M_z(\Omega)$ near the points $\omega_1 = k\Omega$, while the terms with $k < 0$ are nonresonant, while the term with $k = 0$ describes the resonance in a zero effective field: $\omega_1 = 0$. In analogy with the known Hanle effect, we shall henceforth use the designation Hanle resonance for the resonance in zero field.

The values of the terms in formula (1) are determined by the values of the Bessel functions $I_k(\varkappa)$. According to estimates presented below, the argument $\varkappa$ of these functions is a small quantity, $\varkappa = (3-19) \times 10^{-3}$ under our conditions, Using the expansion of the functions $I_k(\varkappa)$ in powers of $\varkappa$ and the known dependence of the optical-detection signal A on M_z ($A \sim N\Gamma_p M_z$), we obtain on the basis of (1) an expression for A:

$$A = A_c \cos \Omega t + A_s \sin \Omega t; \quad (3)$$

$$A_c = \beta \bar{M}_0 N \Gamma_p^2 \frac{\varkappa}{2} \left[-\frac{\omega_1 + \Omega}{(\bar{\Gamma}+\Gamma_p)^2 + (\omega_1+\Omega)^2} + \frac{\omega_1 - \Omega}{(\bar{\Gamma}+\Gamma_p)^2 + (\omega_1-\Omega)^2} \right], \quad (4)$$

$$A_s = \beta \bar{M}_0 N \Gamma_p^2 \frac{\varkappa}{2} \left[\frac{\bar{\Gamma}+\Gamma_p}{(\bar{\Gamma}+\Gamma_p)^2 + (\omega_1+\Omega)^2} - \right. \quad (5)$$
$$\left. - \frac{2(\bar{\Gamma}+\Gamma_p)}{(\bar{\Gamma}+\Gamma_p)^2 + \omega_1^2} + \frac{\bar{\Gamma}+\Gamma_p}{(\bar{\Gamma}+\Gamma_p)^2 + (\omega_1-\Omega)^2} \right].$$

In the derivation of formulas (4) and (5) from (1), we have discarded terms proportional to $\varkappa^3$ and higher powers of $\varkappa$. The coefficients of $\varkappa^2$ turned out to be equal to zero. In formulas (4) and (5), β is the proportionality coefficient, and N is the concentration of the He^4 atoms in the metastable 2^3S_1 state.

It follows from (4) that (at $\varkappa \ll 1$) the in-phase component of the signal should be a sum of a signal having a dispersion shape with center at the point $\omega_1 = \Omega$, and a nonresonant signal that decreases monotonically with increasing ω_1. The experimentally obtained curve 1 of Fig. 2 agrees qualitatively with formula (4). The quadrature component of the signal should according to formula (5), be the sum of a Hanle signal, of a resonant absorption line with center at the point $\omega_1 = \Omega$, and a nonresonant increment that decreases with increasing ω_1. It follows also from (5) that the Hanle signal should be double the first-resonance signal ($\omega_1 = \Omega$), and that the signs of these signals should differ. The experimental curve 2 in Fig. 2 has these properties and can be interpreted as the quadrature component of the signal predicted by formula (5), taken with the minus sign. The minus sign is due to the choice of the absolute value of the phase of the reference voltage in the synchronous detector 11 (Fig. 1). Some deviation of the Hanle signal in Fig. 2 (curve 2) from the theoretical form at low values of H can be attributed to the nonlinearity of the horizontal sweep at small values of U. It follows from (4) and (5) that the swing of the dispersion curve $2A_{c\text{-max}}$ should be equal to the amplitude $A_{s\text{-max}}$ ($\omega_1 = \Omega$) of the first resonance. For curves 1 and 2 of Fig. 2, the ratio of these quantities is 1.04, in good agreement with the theoretical value.

The second-resonance signals ($\omega_1 = 2\Omega$) and the signals of the higher-order resonances, predicted by formula (1), were not observed in the experiment. It follows from (1) that at $\varkappa \ll 1$ the amplitudes of these resonances are much smaller than the amplitudes of the first resonance. For example, the amplitude of the second resonance is proportional to $\varkappa^3$, and the ratio of the amplitude of the second resonance to the amplitude of the first resonance is equal to $\varkappa^2/8$, i.e., under our conditions $(1-50) \times 10^{-6}$. The signal/noise ratio for the signal of the first resonance in the experiment cannot exceed several times 10, and consequently the signals of the second and higher resonances could not be observed.

To verify that the line center U_0 of the observed first-resonance signals indeed corresponds to the resonant value of the field $H_1 = \Omega/\gamma$, we measured the field H_1 as a function of the voltage U at the output of the attenuator. The field H_1 was measured with a calibrated loop antenna located near the absorbing cell. The lower part of Fig. 2 shows the scale of the field H_1, constructed from the results of these measurements. It is seen from Fig. 2 that the value H_{10} corresponding to the center U_0 of the observed resonance line differs somewhat from the theoretical value Ω/γ. The difference amounts to 4.6% and lies within the limits of the measurement errors. The relative error in the measurement of H_1 was 15%. To check, with high accuracy, on the satisfaction of the resonance condition $\omega_1 = \Omega$, we plotted in the same scale (along the x axis) the signals obtained with relaxation modulation and the signals obtained when the pump light was modulated. It is known that when the pump light is modulated at a frequency Ω, resonant signals are observed at $\omega_1 = \Omega$[3]. The experiment with modulation of the pump light was performed with the setup whose block diagram is shown in Fig. 1, except that the modulating voltage of frequency Ω was fed from generator 13 not to generator 12 but to generator 2, which produced the discharge in the pump lamp 1. The measurements have shown that the line center of the signal observed in relaxation modulation coincides with the line center of the signal observed in pump-light modulation within the limits of the measurement accuracy (0.5%).

Interest attaches to the measurement of the constants $\bar{\Gamma}$ and Γ_p in formulas (4) and (5), and to an investigation of their dependence on the intensity of the discharge and of the pump light. The values of $\bar{\Gamma}$ and Γ_p can be obtained from the line width of the observed signals. In the measurement of the line width, the abscissa scale can be

obtained from the shift of the center of the resonance line with changing discharge-modulation frequency. The width ΔH_1 of the resonance line of the quadrature component of the signal of the first resonance, measured at half height, is equal, in accordance with formula (5), to

$$\Delta H_1 = 2\gamma^{-1}(\bar{\Gamma}+\Gamma_p) = \Delta H_1^* + \Delta H_{1p}. \quad (6)$$

One of the terms of (6), namely $\Delta H_{1p} = 2\gamma^{-1}\Gamma_p$, depends on the rate of the light pumping and describes the optical broadening of the resonance line. The other term, $\Delta H_1^* = 2\gamma^{-1}\bar{\Gamma}$, depends on the average relaxation rate $\bar{\Gamma}$ due to the collisions both in the volume of the cell and with the walls of the cell. In addition, a contribution can be made to $\bar{\Gamma}$ also by the inhomogeneity of the radio frequency magnetic field H_1 and of the constant magnetic field H_0. The rate Γ_p of the light pump is directly proportional to the intensity of the light pump. Consequently, the quantity ΔH_1 should depend linearly on the intensity I of the pump light. An experimental check has confirmed the existence of this dependence. Extrapolation of the total line width ΔH_1 to zero value of the intensity of the light pump in accordance with formula (6) makes it possible to find the value of ΔH_1^*.

Figure 3 shows the results of the measurement of ΔH_1^* and ΔH_{1p} as a function of the discharge intensity. The values of ΔH_{1p} were obtained from the relation $\Delta H_{1p} = \Delta H_1 - \Delta H_1^*$. The value of ΔH_1 in this formula was taken from the maximum pump-light intensity. It is seen from Fig. 3 that ΔH_1^* (and consequently $\bar{\Gamma}$) depends on the discharge intensity linearly. This dependence is apparently due to the fact that an increase of the discharge intensity brings about an increase in the discharge, and this leads in turn to an increase in the rate of collision relaxation. The optical broadening ΔH_{1p} (and accordingly Γ_p), as seen from Fig. 3, depends relatively little on the discharge intensity, with ΔH_{1p} decreasing with increasing discharge intensity. This decrease of ΔH_{1p} seems to be connected with the increased absorption of the pump light. The dependence of the absorption $\Delta I/I$ of the pump light on the discharge intensity is shown by curve 1 of Fig. 3.

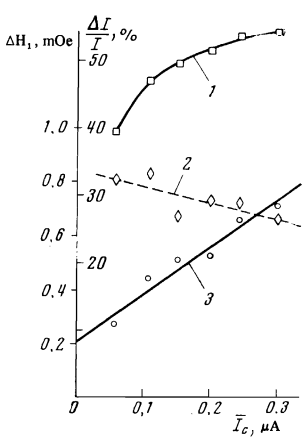

FIG. 3

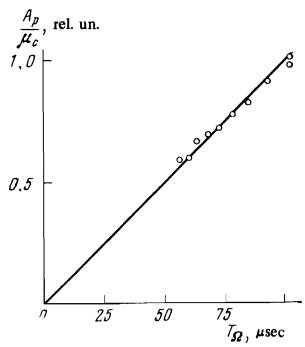

FIG. 4

FIG. 3. Dependence of the relative pump-light absorption $\Delta I/I$ (curve 1) and of the optical contribution ΔH_{1p} (curve 2) and the relaxation contribution ΔH_1^* (curve 3) to the line width of the signal of the first relaxation resonance on the discharge intensity in the cell (P_{He} = 0.8 Torr, $\Omega/2\pi$ = 12.7 kHz).

FIG. 4. Dependence of the ratio of the first-resonance signal A_p to the cell-luminosity modulation depth μ_c on the relaxation modulation period T_Ω ($\bar{I}_c$ = 0.24 μA).

Let us estimate now the relaxation-modulation depth μ obtained in the experiment. The experimental data shown in Fig. 3 indicate that the average relaxation rate $\bar{\Gamma}$ depends on the average discharge intensity $\bar{I}_c$ linearly, $\bar{\Gamma} = A + B\bar{I}_c$.

Consequently, the instantaneous relaxation rate Γ depends on the instantaneous discharge intensity I_c also linearly: $\Gamma = A + BI_c$. If the modulation of the discharge intensity follows the law $I_c = \bar{I}_c(1 + \mu_c \cos\Omega t)$, then the dependence of the relaxation rate on the time should follow formula (2), and the value of μ in formula (2) can be obtained from the relation

$$\mu = \mu_c B\bar{I}_c/\bar{\Gamma}. \quad (7)$$

Formula (7) makes it possible to calculate the relaxation-modulation depth μ if one knows the depth μ_c of the modulation of the cell luminosity. The value of μ_c is calculated from the formula

$$\mu_c = I_{cm}/\bar{I}_c, \quad (8)$$

where I_{cm} is the amplitude of the oscillations of the photoreceiver current of frequency Ω with the pump lamp turned off.

It follows from (7) that $\mu \sim \mu_c$. Inasmuch as the amplitude A_s of the first-resonance signal should be proportional, in accordance with (5), to the relaxation-modulation depth μ, one should expect a linear dependence of A_s on μ_c. The experiments performed have shown that this dependence does indeed take place. It was found experimentally that the modulation depth μ_c of the cell luminosity is directly proportional to the modulation depth m of the electric voltage that maintains the discharge in the cell, and depends in addition on the frequency Ω of the discharge modulation (μ_c changes from 0.34 to 0.24 when $\Omega/2\pi$ changes from 9.8 to 17.7 kHz). From formula (7) at a frequency $\Omega/2\pi$ = 12.7 kHz and m = 1, using the data of Fig. 3 and the measured value μ_c = 0.3, it was found that when I_c changes from 0.06 to 0.30 μA, the relaxation modulation depth μ changes from 0.10 to 0.23. The value of $\kappa = \mu\bar{\Gamma}/\Omega$ changed in this case from 3×10^{-3} to 19×10^{-3}.

In accordance with formula (5), the amplitude of the relaxation-resonance signals should be inversely proportional to the modulation frequency Ω. In the experiment we have indeed observed a decrease of the signals with increasing Ω. However, a change in Ω produced also a change in the relaxation-modulation depth μ (this is evidenced by the dependence of μ_c on Ω). Since $\mu \sim \mu_c$, one should expect on the basis of (5) the ratio of the amplitude A_p of the observed signal to the cell-luminosity modulation depth μ_c to be directly proportional to the discharge-intensity modulation period T_Ω. Figure 4 shows a plot of A_p/μ_c against T_Ω. It is seen from Fig. 4 that the experimental points fit well the theoretical straight line.

In the preceding paper[1] the relaxation resonance in the effective magnetic field was considered only in the case of zero detuning, $\Delta\omega = \omega - \omega_0 = 0$. In the case of nonzero detuning (in analogy with the results of Novikov and Pokazan'ev[3]), one should expect relaxation resonances to be observed when the relaxation modulation frequency Ω coincides with the frequency $\omega_{eff} = \gamma H_{eff}$ and its subharmonics. Here $H_{eff} = [H_1^2 + (\Delta\omega/\gamma)^2]^{1/2}$ is the effective magnetic field. Under the conditions of our experiment, the deviation of the detuning $\Delta\omega$ from zero can lead to a shift of the resonance curves towards

smaller values of the field H_1. These shifts were indeed observed by introducing artificial detuning. At low detuning, the value of the shifts for the first-resonance signal coincided satisfactorily with the expected value $\{\Omega - [\Omega^2 + (\Delta\omega)^2]^{1/2}\}\gamma^{-1}$. At large values of the detuning, a strong broadening of the signals was observed, and their shape was distorted as a result of the poor resolution of the Hanle signal and of the first-resonance signal.

In conclusion, it is the author's duty to thank R. A. Zhitnikov for interest in the work and for stimulating discussions, and also B. N. Sevast'yanov for supplying the helium lamp and the cells.

[1]A. I. Okunevich, Zh. Eksp. Teor. Fiz. 66, 1578 (1974) [Sov. Phys.-JETP 39, 773 (1974)].
[2]R. B. Partridge and G. W. Series, Proc. Phys. Soc., 88, 969 (1966).
[3]L. N. Novikov and V. G. Pokazan'ev, Zh. Eksp. Teor. Fiz. 53, 699 (1967) [Sov. Phys.-JETP 26, 438 (1968)].

Translated by J. G. Adashko.
100